Clinical and molecular characteristics of unicentric mediastinal Castleman disease

Antoine Legras[1,2], Anne Tallet[3], Audrey Didelot[2], Aurélie Cazes[4,5], Claire Danel[4], Angela Hin[5], Raphaël Borie[6], Bruno Crestani[5,6], Yves Castier[5,7], Patrick Bagan[1,8], Françoise Le Pimpec-Barthes[1], Marc Riquet[1], Hélène Blons[2,3]*, Pierre Mordant[5,7]*

[1]Division of Thoracic Surgery and Lung Transplantation, Georges Pompidou European Hospital, [2]INSERM UMR-S1147, CNRS SNC 5014, Saints-Pères Research Center, [3]Division of Molecular Biology, Georges Pompidou European Hospital, Paris-Descartes University, Sorbonne Paris Cité University, Paris, France; [4]Division of Pathology, [5]INSERM UMR-S1152, [6]Division of Pneumology, [7]Division of Thoracic and Vascular surgery, Bichat Hospital, Paris-Diderot University, Paris, France; [8]Division of Thoracic and Vascular surgery, Victor Dupouy Hospital, Argenteuil, France

Contributions: (I) Conception and design: M Riquet, H Blons, P Mordant; (II) Administrative support: None; (III) Provision of study materials or patients: A Legras, A Cazes, C Danel, Y Castier, P Bagan, F Le Pimpec-Barthes, M Riquet, P Mordant; (IV) Collection and assembly of data: A Legras, A Tallet, A Didelot, A Cazes, C Danel, A Hin, Y Castier, P Bagan, F Le Pimpec-Barthes, M Riquet, H Blons, P Mordant; (V) Data analysis and interpretation: A Legras, P Mordant, H Blons, M Riquet, R Borie; (VI) Manuscript writing: All authors; (VII) Final approval of manuscript: All authors.

*These authors contributed equally for the senior authorship.

Correspondence to: Dr. Pierre Mordant, MD, PhD. Division of Thoracic Surgery, Vascular Surgery and Lung Transplantation, Bichat Hospital, 46 rue Henri Huchard, 75018 Paris, France. Email: pierre.mordant@aphp.fr.

Background: Unicentric mediastinal Castleman disease (CD) is a rare condition, poorly characterized due to the small number of cases and the absence of genomic study. We analyzed clinical, radiological, histological and genomic patterns associated with mediastinal CD in a substantial case series.

Methods: We retrospectively reviewed cases of unicentric mediastinal CD managed in 2 French thoracic surgery departments between 1988 and 2012. Clinical, radiological, surgical and pathological data were recorded. On available FFPE blocks we performed mutation screening by next-generation-sequencing, using AmpliSeq™ Cancer Hotspot v2 (Life Technologies) and immunohistochemistry (IHC) (AKT-mTOR pathway).

Results: Eleven patients were identified (mean age 41±15 years, sex-ratio 0.8, median follow-up 78 months). Surgical approach was thoracotomy (n=6), sternotomy (n=4), and VATS (n=1). Additional procedures included thymectomy in three cases, mediastinal lymphadenectomy in two cases, and bilobectomy in one case. One patient presented local relapse as a follicular dendritic cell sarcoma, leading to death 48 months after the first resection. Within 9 patients whose FFPE blocks were available, 2 mutations were found: VHL (p.F119L, 35%, n=1) and JAK3 (p.V718L, 53%, n=1). Phospho-AKT and phospho-mTOR stainings were negative in all cases, whereas phospho-S6RP staining was positive in eight cases, mainly in interfollicular cell cytoplasm.

Conclusions: From this series of patients with unicentric mediastinal CD, we observed 2 cases of potential driver mutations and 8 cases of phospho-S6RP activation not related to AKT-mTOR. Larger studies are required to decipher more precisely the molecular abnormalities and potential therapeutic targets underlying this uncommon condition.

Keywords: Mediastinal tumor; molecular biology; tumor biology; tumor markers; Castleman disease (CD)

2080

Legras et al. Mediastinal Castleman tumor: a molecular view

Introduction

Angiofollicular lymph node hyperplasia was first described by Castleman *et al.* in 1954, and has been then referred to as Castleman disease (CD). The initial description of CD included a series of 13 patients with massive lymph node hyperplasia characterized by germinal center formation and proliferation (1). Histological lesions were separated as hyaline-vascular type or plasma cells type. CD has also been separated between unicentric and multicentric diseases, with major differences in the pathogenesis, clinical presentation, and therapeutic options (2-4). Unicentric or localized CD is less frequent, and less than 300 cases have been published to date, mostly as case reports (5). Lesions are usually hyaline-vascular type. Mediastinum is the main location of localized CD (29%), but a localized CD may be cervical (23%), abdominal (21%), retroperitoneal (16%) and also exceptionally axillary, inguinal or pelvic (5). If the treatment of mediastinal CD is based on radical en-bloc surgical resection, relapse and transformation might occur, urging the need for a better description of disease presentation and associated genomic alterations. However, published series of unicentric mediastinal CD are limited to a small number of patients and lack genomic exploration. We sought to characterize the clinical, radiological, histological and genomic patterns associated with unicentric mediastinal CD in a substantial case series.

Methods

Study design

We set a retrospective study, including all patients operated on for unicentric mediastinal CD in two French thoracic surgery departments from 1988 to 2012. For each patient, clinical, radiological, surgical, and pathological characteristics were collected. The database was approved by the French Committee for Informatics and Liberty (Commission Nationale Informatique et Liberté—CNIL, number 1995655v0). The study protocol was approved by the Institutional Review Board of the French Society of Thoracic and Cardiovascular Surgery (Société Française de Chirurgie Thoracique et Cardio Vasculaire—SFCTCV, number 2016-9-30-10-45-45-MoPi).

Patients' management

All patients underwent complete surgical resection of all macroscopic disease, confirmed through intraoperative frozen section of specimen margins, and definitive examination of the surgical specimen. The diagnosis of CD was then established by a trained pathologist within 1 month after surgery. More recently, all available formalin fixed-paraffin embedded (FFPE) blocks were retrieved for diagnosis confirmation and additional studies including next generation sequencing (NGS) and immunohistochemistry (IHC).

Sequencing

After morphological control of the quality of the tumor sampling, DNA was extracted using the Maxwell® 16 FFPE Plus LEV DNA Purification Kit (Promega Corporation, Madison, WI) and quantified using Qubit™ fluorometric quantitation device (Thermo Fisher Scientific, France). Paraffin-embedded samples were characterized using NGS (AmpliSeq™ Ion Torrent, Life Technologies) designed to amplify small DNA fragments. Multiplex PCR library were prepared using the AmpliSeq™ Cancer Hotspot v2 (Life Technologies) covering more than 2800 COSMIC hotspot mutations within the following 50 genes (*SMARCB1*, *RB1*, *TP53*, *ERBB4*, *FBXW7*, *BRAF*, *TP53*, *KIT*, *GNAS*, *HRAS*, *EGFR*, *PDGFRA*, *PIK3CA*, *CDKN2A*, *ERBB2*, *ABL1*, *JAK2*, *KRAS*, *NRAS*, *NOTCH1*, *ATM*, *FGFR1*, *STK11*, *PTPN11*, *APC*, *SMAD4*, *PTEN*, *SMO*, *CTNNB1*, *RET*, *IDH2*, *SRC*, *EZH2*, *VHL*, *MPL*, *NPM1*, *FLT3*, *FGFR3*, *CDH1*, *KDR*, *HNF1A*, *MLH1*, *ALK*, *IDH1*, *GNAQ*, *AKT1*, *JAK3*, *FGFR2*, *GNA11*, *MET*, *CSF1R*, *CDKN2A*) and Ion AmpliSeq™ library kit V2. Libraries were equalized using ion library equalizer kit (Life Technologies) (6). Quality control was performed using an Agilent 2100 Bioanalyser equipment (Agilent Technologies, USA). Clonal amplification was done on the Ion Chef™ System (ION P1 HI-Q CHEF, ION PI CHIP KITV3) and sequencing was performed on a Ion Proton™ system. Data were analyzed by the Torrent Suite 4.4.3 and variants annotated with Safir2report tool. Variants detection threshold was 2%, minimal deepness for negative results was 300X. Called variants underwent subsequent quality control taking into account the coverage of each amplicon (≥50), the variant quality score and the allele frequency (≥5%). Amplicons list is available at www.thermofisher.com. The identification of gene amplification was performed with an R-tool. Suspected mutations were controlled on Alamut® Visual (Interactive Biosoftware, Rouen, France). NGS results were validated by independent methods using Sanger sequencing or allele-specific real time PCR (for *KRAS* and *NRAS*).

IHC

IHC was performed on fresh 5-µm sections from FFPE blocks on Leica BOND-MAX (Leica Biosystems, Buffalo Grove, IL, USA) automated staining system, in the presence of appropriate controls. Briefly, unstained slides were deparaffinized and subjected to antigen retrieval in a pH=9 buffer, according to manufacturer's recommendations. Primary antibodies were purchased from Cell Signaling Technology (Danvers, MA, USA). Phospho-mTOR (Ser2448), Phospho-S6RP (Ser235/236) and Phospho-AKT (D9E) were used at 1:50, 1:100 and 1:40 dilutions respectively. Revelation was performed with Leica BOND-MAX (Leica) detection kits according to standard manufacturer's protocol. A qualified pathologist (AC) analyzed slides, blinded from clinical characteristics and NGS results.

Statistical analysis

Categorical variables were described as count and proportion. Continuous variables were described as mean and standard deviation. Follow-up information was obtained from the hospitals case records. The main outcome was overall survival, defined as the time interval between the date of operation and the date of death or the last follow-up visit for censored patients. Mean follow-up duration was 78±98 months. All statistical analyses were performed using Excel software (Microsoft, Redmond, WA, USA).

Results

Patients

Eleven patients were operated on between 1988 and 2012, and accounted for the study group. Clinical characteristics are described in *Table 1*. Mean age was 41±15 (range, 17–69) years, sex ratio was 0.8. Pemphigus occurred in 2 patients (cases #2 and #3), both of which reported atopic background. In case #2, antinuclear factor was positive (1/600, anti-DNA 800ui). In case #3, lymphopenia, hypereosinophilia (2,000/mm^3) and anti-intercellular substance and anti-desmoglein-3 antibodies were found. Biological characteristics were otherwise normal for all the patients.

Imaging

Results of chest CT-scan are summarized in *Table 1*. Interstitial syndrome was associated with the mediastinal tumor in cases #2 and #4, one of them presenting with pemphigus (#2). Bronchial endoscopy was normal in six cases and showed extrinsic bronchial compression in four cases. PET-CT was performed in two patients and showed no hypermetabolism of the tumor. *Figure 1* shows representative chest X-rays and CT-scan selected from cases #1, #3 and #5.

Surgical management

Surgical management and postoperative course are described in *Table 1*. The surgery included the complete surgical resection of the mediastinal tumor in all cases. Associated resection included: radical thymectomy in 3 cases (#5, #6 and #9) of anterior mediastinal location; mediastinal lymphadenectomy in case #11 of right para-tracheal mass and sub-carinal satellite adenomegaly; inferior bilobectomy and mediastinal lymphadenectomy in case #10 of hilar location. Complete surgical resection was achieved in all cases. Mean postoperative hospital length of stay was 7±3 (range, 4–15) days. No in-hospital mortality was noticed.

Histology

We observed constantly a homogeneous mass of lymphoid tissue, sprinkled with nodules or follicles and interfollicular spaces (*Figure 2*), as previously described in CD (5). The nodules were made by a germinal center, surrounded by the hyperplastic mantle. No lymphatic sinus was observed. Germinal centers were active or regressed, due to depletion of their centrofolicular lymphoid cells. Perivascular calcifications were found in case #1, and an inflammatory pseudo-tumor with fusiform cells was found in case #3. Adjacent adenomegalies showed only anthracosis or sinus histiocytosis without specific involvement.

Adjuvant treatments and follow-up

Adjuvant immune-suppressive therapy was administered in 2 patients (#2 and #3). The latest (case #3) presented a myasthenia 2 years later, leading to the discovery of a local relapse. She was operated again and final pathological examination concluded to follicular dendritic cell sarcoma. She received adjuvant radiation therapy, presented loco regional relapse (mediastinum and pleura, *Figure 1F*), and ultimately died 4 years after initial resection. After a median follow-up of 78 months, no other patient presented with disease recurrence or specific mortality. The overall 5-year survival rate was 91% (10/11).

2082

Legras et al. Mediastinal Castleman tumor: a molecular view

Table 1 Clinical, tomodensitometry characteristics, surgical management and outcome (study group, n=11)

Variable	N
Clinical characteristics	
Age (years)	
Mean ± SD	41±15
Range	17–69
Sex-ratio	0.8
Tobacco use	1
Allergic manifestations	3
Neurofibromatosis	1
Drepanocytosis	1
Symptoms	
Dyspnea	4
Pain	2
Dysphagia	2
Cough	2
Pemphigus	2
Weight loss	1
Fever	1
SVC syndrome	1
Mouth aphthosis	1
Fortuitous diagnosis	3
Tomodensitometry characteristics	
Tumor size (mm)	
Mean ± SD	57±13
Range	40–80
Tumor location	
Sub-carinal	3
Right para-tracheal	2
Left para-tracheal	2
Anterior	2
Posterior	1
Hilar	1
Tumor characteristics	
Calcifications	3
Contrast enhancement	2
Central necrosis	1

Table 1 (*continued*)

Table 1 (*continued*)

| Variable	N
Associated CT abnormalities	
Interstitial syndrome	2
Oesophageal compression	2
Vena cava compression	2
Surgical management	
Operative approach	
Postero-lateral thoracotomy	6
Full sternotomy	2
Partial sternotomy	2
VATS	1
Additional procedures	
Mediastinal lymphadenectomy	2
Thymectomy	3
Preoperative tracheostomy	1
Inferior bilobectomy	1
Outcome	
Postoperative course	
Pneumonia	1
Atelectasis	1
Transient phrenic palsy	1
Mortality	0

SVC, superior vena cava; VATS, video-assisted thoracoscopic surgery.

Sequencing

For 9 patients, FFPE blocks were available and NGS was performed. Twelve variants were suspected for somatic mutation after Alamut® Visual control (*Table 2*), distributed in 5 cases. After Sanger sequencing, only 2 mutations were confirmed: *VHL* (c.355T>C; p.F119L; 35%) in case #11, and *JAK3* (c.2152G>C; p.V718L; 53%) in case #1 (*Figure 3*). No gene amplification was detected in this series using targeted NGS data.

IHC

For the nine patients whose FFPE blocks were available, IHC was also performed (*Table 3*). Phospho-S6RP showed frequently positive staining (n=8; + to +++) in
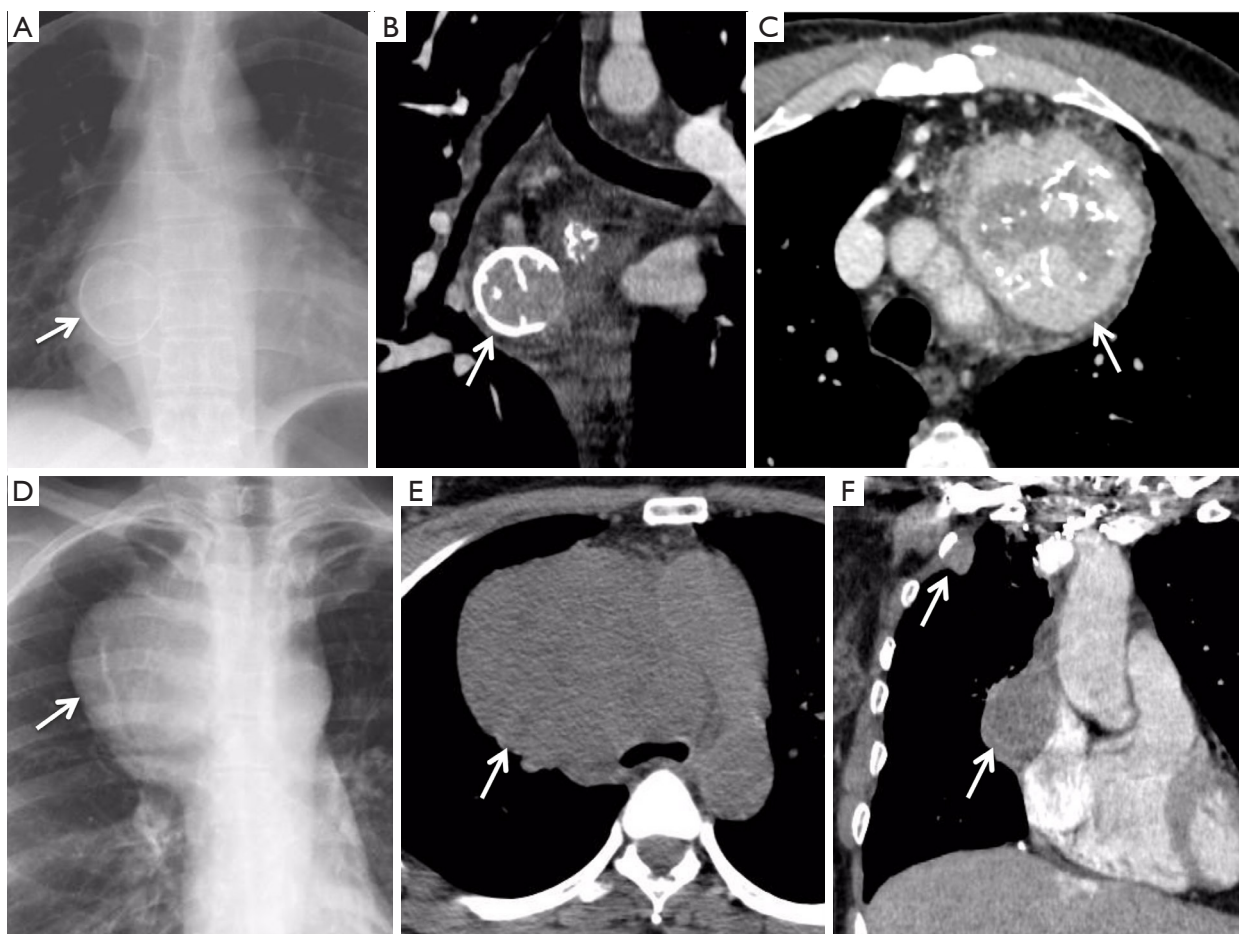
Figure 1 Representative chest X-rays and CT-scan selected from cases #1, #3 and #5. (A) Case #1, chest X-rays; (B) case #1, CT-scan, frontal section; (C) case #5, CT-scan, transversal section, showing tumor heterogeneity and calcifications; (D) case #3, chest X-rays before surgery; (E) case #3, CT-scan, transversal section, before surgery; (F) case #3, CT-scan, frontal section, showing mediastinal and pleura sarcoma relapse. Arrows indicate tumors.

the interfollicular zone, and also in the germinal centers in most cases, but with less stained cells (n=7; +/− to ++; *Figure 2B*). Three cases presented phospho-S6RP staining on microvascular endothelial cells (case #6, *Figure 2C*). The staining of a hyperplastic lymphadenopathy used as a reference for maximal staining (++++) is shown in *Figure 2D*. Phospho-AKT and phospho-mTOR were negative in all cases including the hyperplastic lymphadenopathy.

## Discussion

Main results reminder

In this retrospective series of 11 patients with unicentric mediastinal CD, we reported complete surgical resection

in all cases, local relapse and transformation as follicular dendritic cell sarcoma leading to death in one case. We also observed two cases of mutation involving *VHL* (p.F119L) and *JAK3* (p.V718L) and eight cases of mTOR-independent S6RP activation.

CD

Inappropriate inflammatory response might be the core of the genesis of CD (7). However, the exact pathophysiology of localized CD remains unclear, as its rarity hinder basic investigations. Standard treatment of mediastinal CD relies on radical en-bloc surgical resection. Relapse is rare and usually local with overall 5-year survival >95% in case of complete resection (5). Optional treatments include

2084

Legras et al. Mediastinal Castleman tumor: a molecular view
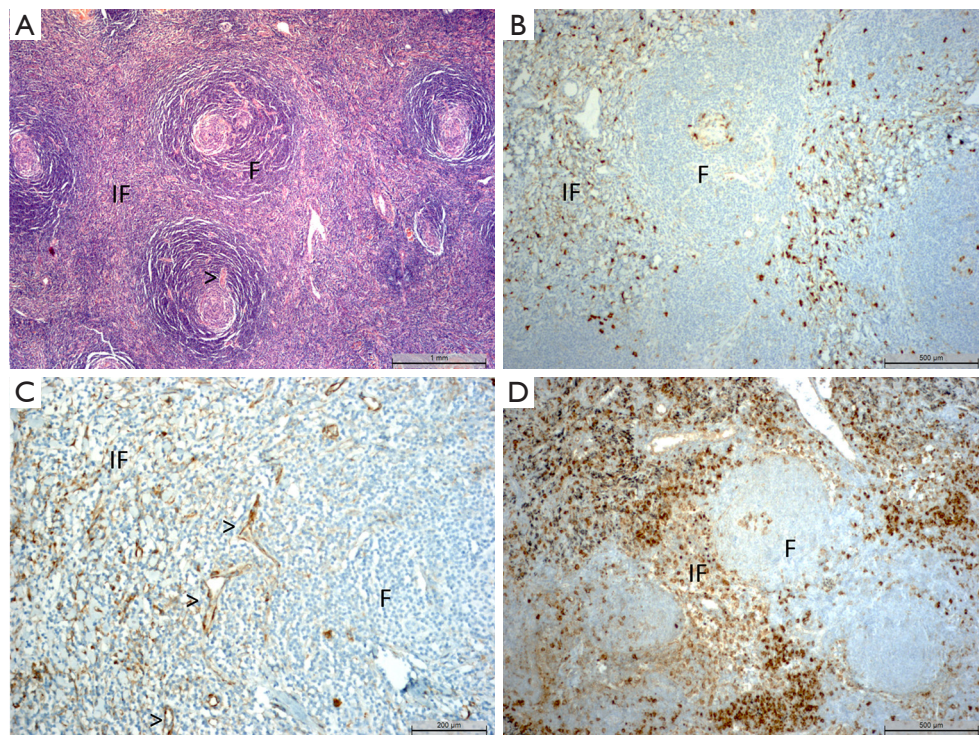
Figure 2 Pathology and immunohistochemistry. (A) Characteristic aspect of a Castleman disease (case #9); follicles (F) and interfollicular spaces (IF), follicle containing a germinal center, surrounded by the hyperplastic mantle (typical onionskin aspect) with blood vessels (>) penetrating radially the germinal center. Hematoxylin-Eosin-Safran staining, obj×10; (B) phospho-S6RP staining in the interfollicular zone and in the germinal center (case #11, obj×10); (C) phospho-S6RP staining within endothelial cells (case 6, obj×20); (D) phospho-S6RP staining in a hyperplastic lymphadenopathy (control).

Table 2 List of variants identified with next generation sequencing on Ion Proton™ system (patients with available FFPE blocks, n=9)

Patient #	Gene	Depth (reads)	Frequency (%)	Quality score	cDNA change	Protein change
4	NRAS	141	12	73	c.34G>A	p.G12S
4	STK11	158	7	20	c.502C>T	p.H168Y
4	KRAS	132	8	37	c.183A>C	p.Q61H
6	JAK2	219	6	33	c.1853G>A	p.C618Y
6	SMAD4	289	6	29	c.370G>A	p.D124N
10	MLH1	120	6	54	c.1240G>A	p.E414K
10	AKT1	112	11	52	c.136G>A	p.D46N
10	ERBB4	86	9	32	c.1753G>A	p.D585N
11	VHL	23	35	55	c.355T>C	p.F119L
11	HRAS	50	8	19	c.37G>A	p.G13S
11	STK11	80	9	12	c.144_145insG	p.K48fs
1	JAK3	600	53	3,565	c.2152G>C	p.V718L

The quality column reflects a quality metric of 'Phred-like' scores to determine the accuracy of calling bases in the sequence.
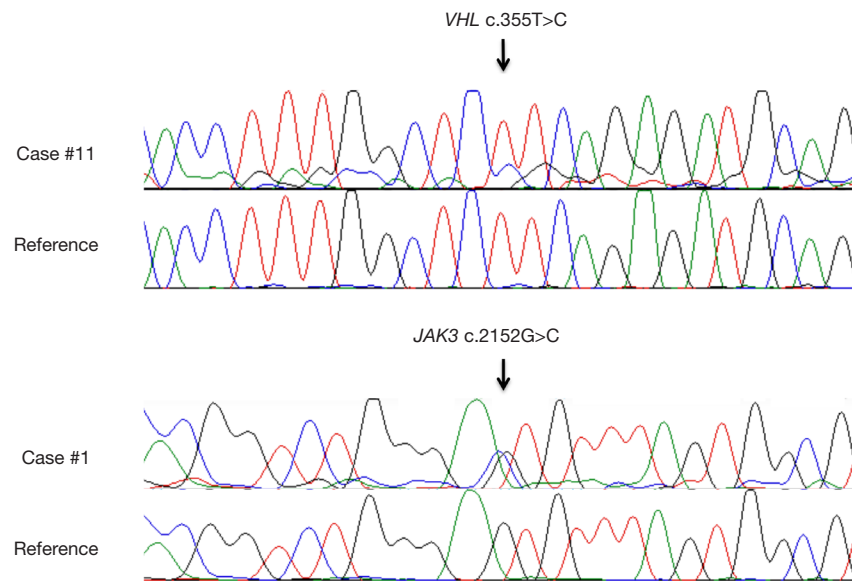
Figure 3 Sanger mutation confirmation: *VHL* (p.F119L) in case #11 and *JAK3* (p.V718L) in case #1.

Table 3 Immunostaining for phospho-S6RP (patients with available FFPE block, n=9)

| Patient # | Interfollicular zone | Follicular zone | | Microvascular endothelial cells |
		Germinal centers	Mantle and marginal zone	
1	+++	+/–	+/–	0
2	+++	++	+/–	0
3	++	0	0	0
4	+	+	0	0
6	+	+	0	+++
8	++	+/-	0	0
9	++	0	0	+++
10	0	+	0	0
11	+++	++	0	+
Control	++++	++	+/–	–

A hyperplastic lymphadenopathy was used as an external control, to compare the staining.

preoperative embolization to limit intra-operative bleeding and adjuvant radiation therapy in case of incomplete resection (8,9). Radiotherapy has also been offered in a curative intent (10), but the experience remains limited and its long-term efficacy warrants confirmation. Furthermore, CT-guided or EBUS-guided biopsy of localized mediastinal mass performed before radiotherapy might be misleading, whereas complete surgical resection allows the exact diagnosis together with adequate treatment and long-term survival of the vast majority of patients with unicentric mediastinal CD.

Surgical management

Some precautions might be helpful when planning surgery for CD. Paraneoplastic pemphigus may concern <10%

2086

Legras et al. Mediastinal Castleman tumor: a molecular view

of cases, associated with adverse outcome mainly due to mucous membrane involvement (11). In our series, pemphigus was present in two cases, associated with bronchiolitis and risk of transient postoperative worsening of the dyspnea and broncho-pleural fistula in case of lung resection. For all these reasons, the adequate management of bronchiolitis or pemphigus is mandatory before planning the surgical resection of underlying unicentric mediastinal CD. Neoadjuvant therapy with intravenous immunoglobulin or rituximab has been suggested to reduce the risk of post-operative flare of paraneoplastic pemphigus (12).

Previous reports described unicentric CD as a localized disease without any lymphatic spreading (5). However, the accuracy of CT and PET-CT has not been assessed in the lymphatic extension of unicentric mediastinal CD. Interestingly, mediastinal lymphadenectomy was performed in two cases of our series. For these two patients, all resected lymph nodes were free of tumor. Furthermore, the only local recurrence reported in our series occurred in the bed of the first tumor, and not in an adjacent lymph node stations. Thus, the rational and benefit of lymphadenectomy might be discussed. It is now our policy to perform lymphadenectomy of adjacent stations in the absence of diagnosis at the time of surgery, whereas it is not mandatory when the diagnosis of unicentric mediastinal CD has been confirmed preoperatively.

Mutational analyses

In our series, NGS followed by Sanger analysis revealed two mutations. The *VHL* mutation (p.F119L; allelic ratio 35%) is a loss-of-function mutation, known as disruptive, previously described in renal cell carcinoma (13-16). *VHL* is the causative gene for both von Hippel-Lindau disease and sporadic clear-cell renal cancer. The 96-122 domain is disproportionately affected by substitution mutations and contributes importantly to VHL tumor suppressor activity (17). Furthermore, the p.F119 is one of the 4 amino-acid of the aromatic tetrahedron core of the VHL protein (18). Sequencing depth was only 23 reads, reflecting the poor technical conditions (*Table 2*). However, allelic ratio was high and the mutation was observed in both strands. Furthermore, the mutation was confirmed with Sanger technique.

The *JAK3* mutation (p.V718L; allelic ratio 53%) affects an amino-acid within the pseudo-kinase domain JH2. Mutations of *JAK3* (A572V, A573V and V722I) were

described in extranodal natural killer/T-cell lymphoma and play fundamental roles in development of natural killer/T-cell lymphoma (19,20). These substituted amino acids are involved in the C helix (A573) and in the kinase fold F helix (V722), suggesting that these mutations disrupt an important autoregulatory interaction between the JH2 and JH1 domains (19). *JAK3* mutations were associated with phosphorylation of JAK3 tyrosine 980 and activation of downstream signaling, including STAT, AKT, and ERK pathways, responsible for proliferation and invasiveness (19). *JAK3* mutations have been found in other hematologic malignancies at lower frequencies, especially in T-lymphoid and myeloid malignancies (20). In clinical settings, JAK3 inhibitors have been applied as immunomodulators in rheumatoid arthritis and might be a therapeutic option for some CD (21). Curiously here, the allelic ratio reached 50%, asking for germline mutation, previously described in ClinVar (https://www.ncbi.nlm. nih.gov/clinvar/). Interestingly, the former mutation (*VHL* p.F119L) has been involved in abnormal angiogenesis with constitutional activation of the hypoxia inducible factor (HIF) pathway and subsequent increased expression of angiogenic and growth factors (vascular endothelial growth factor and platelet-derived growth factor B chain), that contribute to the growth and proliferation of tumor cells (22), whereas the latter mutation (*JAK3* p.V718L) has been involved in extranodal natural killer/T-cell lymphoma, encompassing two important parts of CD histology. Whether each mutation is limited to only part of the tumor (i.e., VHL around prominent blood vessels and JAK3 in lymphoid nodules), could only be determined after specimen microdissection that has not been performed here. These mutations should be screened in CD to estimate the impact of these alterations in CD genesis.

mTOR pathway

We focused on AKT-mTOR-S6RP pathway, as it has been reported to been activated in mantle cell lymphoma, that shares some histologic features with unicentric CD. This pathway is also interesting as a potential therapeutic target, given that numbers of inhibitors have already been approved in other conditions. Our IHC findings were limited to an mTOR-independent activation of S6RP, mainly in the interfollicular space. This pattern of strong expression of phospho-S6RP in T interfollicular zone and scarce positive cells in B follicular zones is reminiscent of the pattern observed in a hyperplastic lymph node and

suggests an expression by T lymphocytes. Whether this activation of S6RP is only a marker of cell proliferation, or a direct consequence of activated upstream pathways such as MEK/ERK or STAT, should be deciphered more precisely.

Study limitations

FFPE blocks were frequently old for these patients, with half of them operated more than 10 years ago. To ensure good results reproducibility, DNA libraries were repeated 3 times and sequenced separately in the Ion Proton™ system. All the BAM files were analyzed on Alamut® Visual and variants were selected for confirmation with Sanger technique. Only 2 mutations were confirmed with this gold standard technique, however for allelic ratios <5%, the Sanger technique may be not sensitive enough (23). Thus, some of the mutations found with NGS (*Table 2*) but not confirmed using Sanger technique may be nevertheless present, with low allelic ratio (6–12%). Also, some other mutations might have been missed due to DNA amplification and sequencing difficulties (low NGS coverage). Finally, the functional impact of these mutations at the cellular level should be deciphered more precisely. Also, activated pathways associated to S6RP activation should be investigated, such as MEK/EKK and STAT, in further studies.

Conclusions

In conclusion, from this series of patients with unicentric mediastinal CD, we observed two cases of potential driver mutations (*VHL* p.F119L and *JAK3* p.V718L) and 6 cases of phospho-S6RP activation (not related to AKT-mTOR pathway). Larger studies are required to decipher more precisely the molecular abnormalities and potential therapeutic targets underlying this uncommon condition.

Acknowledgements

None.

Footnote

Conflicts of Interest: The authors have no conflicts of interest to declare.

Ethical Statement: The database was approved by the French

Committee for Informatics and Liberty (Commission Nationale Informatique et Liberté—CNIL, number 1995655v0). The study protocol was approved by the Institutional Review Board of the French Society of Thoracic and Cardiovascular Surgery (Société Française de Chirurgie Thoracique et Cardio Vasculaire—SFCTCV, number 2016-9-30-10-45-45-MoPi). The study outcomes will not affect the future management of the patients included in the study.

References

1. Castleman B, Iverson L, Menendez VP. Localized mediastinal lymphnode hyperplasia resembling thymoma. Cancer 1956;9:822-30.
2. Dupin N, Diss TL, Kellam P, et al. HHV-8 is associated with a plasmablastic variant of Castleman disease that is linked to HHV-8-positive plasmablastic lymphoma. Blood 2000;95:1406-12.
3. Dossier A, Meignin V, Fieschi C, et al. Human herpesvirus 8-related Castleman disease in the absence of HIV infection. Clin Infect Dis 2013;56:833-42.
4. Borie R, Cadranel J, Guihot A, et al. Pulmonary manifestations of human herpesvirus-8 during HIV infection. Eur Respir J 2013;42:1105-18.
5. Talat N, Belgaumkar AP, Schulte KM. Surgery in Castleman's disease: a systematic review of 404 published cases. Ann Surg 2012;255:677-84.
6. Pécuchet N, Legras A, Laurent-Puig P, et al. Lung cancer molecular testing, what role for next generation sequencing and circulating tumor DNA. Ann Pathol 2016;36:80-93.
7. Casper C. The aetiology and management of Castleman disease at 50 years: translating pathophysiology to patient care. Br J Haematol 2005;129:3-17.
8. Neuhof D, Debus J. Outcome and late complications of radiotherapy in patients with unicentric Castleman disease. Acta Oncol. 2006;45:1126-31.
9. Sanchez-Ros-Sanchez A, Infante-Cossio P, Gonzalez-Garcia A, et al. Preoperative embolization for the treatment of cervical Castleman disease. J Craniofac Surg 2012;23:e257-9.
10. Noh OK, Lee S-W, Lee JW, et al. Cases report of unicentric Castleman's disease: revisit of radiotherapy role. Radiat Oncol J 2013;31:48-54.
11. Dong Y, Na J, Lv J, et al. Clinical and laboratory characterization of a large cohort of patients with Castleman disease retrospectively collected from a single

center. Leuk Lymphoma 2009;50:1308-17.

12. Wang J, Zhu X, Li R, et al. Paraneoplastic pemphigus associated with Castleman tumor: a commonly reported subtype of paraneoplastic pemphigus in China. Arch Dermatol 2005;141:1285-93.

13. Brauch H, Weirich G, Hornauer MA, et al. Trichloroethylene exposure and specific somatic mutations in patients with renal cell carcinoma. J Natl Cancer Inst 1999;91:854-61.

14. Muscarella LA, D'Agruma L, la Torre A, et al. VHL gene alterations in Italian patients with isolated renal cell carcinomas. Int J Biol Markers 2013;28:208-15.

15. Sato Y, Yoshizato T, Shiraishi Y, et al. Integrated molecular analysis of clear-cell renal cell carcinoma. Nat Genet 2013;45:860-7.

16. Togo Y, Yoshikawa Y, Suzuki T, et al. Genomic profiling of the genes on chromosome 3p in sporadic clear cell renal cell carcinoma. Int J Oncol 2016;48:1571-80.

17. Cohen HT, Zhou M, Welsh AM, et al. An important von Hippel-Lindau tumor suppressor domain mediates Sp1-binding and self-association. Biochem Biophys Res Commun 1999;266:43-50.

18. Shmueli MD, Schnaider L, Rosenblum D, et al. Structural insights into the folding defects of oncogenic pVHL lead to correction of its function in vitro. PloS One 2013;8:e66333.

19. Bouchekioua A, Scourzic L, de Wever O, et al. JAK3 deregulation by activating mutations confers invasive growth advantage in extranodal nasal-type natural killer cell lymphoma. Leukemia 2014;28:338-48.

20. Sakata-Yanagimoto M, Enami T, Yokoyama Y, et al. Disease-specific mutations in mature lymphoid neoplasms: recent advances. Cancer Sci 2014;105:623-9.

21. Van Vollenhoven RF, Fleischmann R, Cohen S, et al. Tofacitinib or adalimumab versus placebo in rheumatoid arthritis. N Engl J Med 2012;367:508-19.

22. Shenoy N, Pagliaro L. Sequential pathogenesis of metastatic VHL mutant clear cell renal cell carcinoma: putting it together with a translational perspective. Ann Oncol 2016;27:1685-95.

23. Gao J, Wu H, Shi X, et al. Comparison of next-generation sequencing, quantitative PCR, and sanger sequencing for mutation profiling of EGFR, KRAS, PIK3CA and BRAF in Clinical Lung Tumors. Clin Lab 2016;62:689-96.